MAGNETIC RESONANCE IMAGING FEATURES OF INTRAVENTRICULAR EPENDYMOMAS IN FIVE CATS

ANTONIA DEJESUS, ELI B. COHEN, EVELYN GALBAN, JANTRA NGOSUWAN SURAN

Intraventricular ependymoma is a rare type of feline intracranial neoplasia and published information on magnetic resonance imaging (MRI) characteristics is currently lacking. The purpose of this retrospective case series study was to describe the clinical and MRI characteristics of histopathologically confirmed intraventricular ependymomas in a group of cats. Five cats met inclusion criteria. In relation to normal gray matter, ependymomas appeared hyperintense on T2W, T2W-FLAIR, PD, and DW-EPI images; isointense on ADC images; and had subtle to strong contrast enhancement. Some variability was seen on T2∗GRE and on T1W images with masses being isointense to hyperintense. Four ependymomas were small and homogeneous, and one was centrally cavitated. All cats had obstructive hydrocephalus, transtentorial herniation, and foramen magnum herniation. Perilesional edema was identified in most cats but was questionable in one. Intraventricular ependymoma should be considered as a differential diagnosis for cats with this combination of MRI signs.

Key words: cat, ependymoma, feline, intraventricular, MRI.

Introduction

EPENDYMOMAS ARE GLIAL TUMORS arising from the ependymal cells lining the ventricular system and have been reported as a rare form of intracranial neoplasia in cats.[1–5] Among other intracranial neoplasms, the incidence for ependymomas has been described as up to 2.8%.[3,6] Like other intracranial tumors, ependymomas are often benign in that they do not tend to metastasize, however their location and growth can result in significant secondary deleterious effects by causing vascular compromise and compression of the surrounding parenchyma.[1] Prognosis for feline ependymomas is generally poor. The mean age of cats diagnosed with intracranial neoplasms was previously reported as 11.3 ± 3.8 years (range 0.5–21.5 years).[3] Cats with ependymomas were found to be significantly younger (8.2 ± 3.3 years) in comparison to those with meningiomas (12.2 ± 3.3 years).[3,5] A mild bias for female cats was seen with ependymomas in one study, a correlation with breed was not established.[5] Surgical excision with resolution of clinical signs has been reported in one cat with a third ventricular ependymoma.[7]

Ependymomas can be histopathologically classified into four subtypes (cellular, papillary, tancytic, and clear cellular), although some show evidence of more than one subtype.[5,8] Furthermore, ependymomas can either be benign or malignant. Malignant characteristics include anaplasia, a high mitotic rate, necrosis, and invasion of neighboring parenchyma.[1,9] In humans, ependymomas can occur in any age group, but are more commonly seen in children with no clear sex predilection. In humans, ependymomas occur slightly more frequently infratentorially (60%) than supratentorially (40%), with supratentorial ependymomas being more often intraparenchymal/intra-axial than intraventricular.[8] In children, masses tend to be infratentorial, occurring in the posterior fossa, while supratentorial masses are more common in adults.[8] A supratentorial intraventricular location is more frequently reported in dogs and cats.[1–3,5–7,10,11] In cats, most ependymomas have been reported to originate from the walls of the lateral and third ventricles.[2,3,5–7] Ependymomas have been less frequently reported to occur in the subarachnoid space, fourth ventricle, mesencephalic aqueduct, and central canal of the spinal cord.[5]

To the authors' knowledge there are no prior reports on the magnetic resonance imaging (MRI) characteristics for feline ependymomas. The purpose of this study to

From the BluePearl Veterinary Partners, New York, NY 10019 (DeJesus), The Department of Molecular Biomedical Sciences, NC State, College of Veterinary Medicine, Raleigh, NC 27607 (Cohen), and The Department of Clinical Studies-Philadelphia, School of Veterinary Medicine, University of Pennsylvania, Philadelphia, PA 19104 (Galban, Suran).

Presented in abstract form at the 2015 American College of Veterinary Radiology annual scientific conference in Minneapolis, MN, 2015.

Address correspondence and reprint requests to Dr. Jantra Suran, Department of Radiology, School of Veterinary Medicine, University of Pennsylvania, 3900 Delancey St., Philadelphia, PA 19018. E-mail: jsuran@vet.upenn.edu

Received June 9, 2016; accepted for publication November 14, 2016.
doi: 10.1111/vru.12464

describe the MRI characteristics of confirmed intraventricular ependymomas in a group of cats.

Materials and Methods

Medical records were searched for cats that were diagnosed with an intraventricular ependymoma at NC State University between 2005 and 2014 and at the University of Pennsylvania between 2007 and 2014. Cases were included if an antemortem brain MRI was performed and histopathologic diagnosis of an ependymoma from a surgical biopsy or necropsy was available. Images were reviewed independently by two board-certified veterinary radiologists (J.S., E.C.); in the instance of conflicting opinions, images were reevaluated and a consensus was reached. The MRI characteristics of the masses evaluated included lesion location, shape, signal intensity relative to normal gray matter (hyperintense, isointense, hypointense), degree of contrast enhancement (none, mild, strong), pattern of contrast enhancement (homogeneous, heterogeneous), presence of intralesional cavitations, degree of cerebrospinal fluid (CSF) suppression on T2W-FLAIR, secondary effects of the mass including brain herniation, ventricular dilation, and peritumoral edema. Signalment, clinical signs, laboratory findings, and histopathologic diagnosis were also recorded.

Results

Cats

At NC State University, out of 228 feline brain MRIs, seven cats had an intraventricular mass, and three cats met the inclusion criteria. At the University of Pennsylvania, out of 171 feline brain MRIs, five cats had an intraventricular mass, and three cats met the inclusion criteria. Of the six cats diagnosed with an ependymoma, one case was excluded due to having an incomplete imaging study of the lesion, limited to proton density (PD) and T2-weighted images (T2W). A full necropsy was performed in 4/5 cats. The brain of cat #3 was examined histopathologically postmortem in conjunction with an antemortem surgical biopsy. The cats were 4, 4.5, 5, 9, and 10 years old (mean age 6.5 years old). Three cats were spayed females and two were castrated males. Three of the cats were domestic shorthaired cats and two were domestic longhaired cats. Demographic information and clinicopathologic findings are summarized in Appendix 1.

Clinical Findings

Prior to presentation, the duration of owner-reported clinical signs ranged from less than 1 day to 2 months. Neurologic signs at the time of presentation included circling/aimless walking, vestibular ataxia, changes in behavior and mentation, positional nystagmus, proprioceptive and cranial nerve deficits, and seizures. Physical examinations were otherwise normal. Blood work, including a complete blood count, serum biochemistry panel, and when available, infectious disease tests, were unremarkable. Thoracic (4/5 cats) and cervical (1/5 cats) radiographs were normal. Abdominal ultrasound (2/5 cats) identified mild hepatic changes (subjectively hypoechoic (1/2) or hyperechoic (1/2)). Fine needle aspirates of the liver in both cases were cytologically normal. Prior to MRI, cat #1 went into respiratory arrest, and was subsequently resuscitated, intubated, and provided with mechanical-assisted ventilatory support with subsequent imaging.

TABLE 1. Magnetic Resonance Imaging Sequences and the Number of Cats in which Each Sequence was Performed

	Image plane		
Sequence	Transverse	sagittal	Dorsal
T1W precontrast	5/5	2/5	3/5
T1W postcontrast	5/5	4/5	5/5
T2W	5/5	3/5	2/5
T2W-FLAIR	5/5		
T2*GRE	4/5		
DW-EPI	3/5		
ADC	3/5		
PD	2/5		

FLAIR, fluid attenuation inversion recovery; DW-EPI, diffusion weighted echo-planar images; ADC, apparent diffusion coefficient images; GRE, gradient echo; PD, proton density.

Magnetic Resonance Imaging Findings

For all included cats, MRI was performed using 1.5 T MRI units (GE Medical System, Milwaukee, WI; Siemens Medical Solutions, Malvern, PA) with the patient in sternal recumbency under general anesthesia. All cases included T1-weighted images (T1W) before and immediately after intravenous bolus administration of gadopentetate dimeglumine at 0.2 mL/kg of body weight (Magnevist, Berlex Imaging, Wayne, NJ) in a transverse plane, T2W in a transverse plane, and T2-weighted fluid attenuated inversion recovery images (T2W-FLAIR) in a transverse plane. Additional sequences performed are listed in Table 1. Sequence parameters are summarized in Table 2. All MRI studies were performed within 1 day of presentation. The MRI findings are summarized below and further details for individual patients can be found in Appendix 2.

All (5/5) masses in this study were intraventricular, being either ovoid (4/5) or spherical (1/5) in shape. The masses were hyperintense relative to normal gray matter on T2W, PD, and T2W-FLAIR images, and isointense to hyperintense relative to normal gray matter on T1W images (Fig. 1). Strong, homogeneous contrast enhancement was present in 4/5 cats, with one cat (cat #5) having mild,

Table 2. Magnetic Resonance Imaging Sequence Parameters Used for Five Cats with Intraventricular Ependymomas

Sequence	Repetition time (ms)	Echo time (ms)	Inversion time (ms)
T1W precontrast	317–750	10–23	
T1W postcontrast	317–750	10–23	
T2W	3800–6900	57–104	
T2W-FLAIR	8002–9000	78–131	2000–2500
T2*GRE	367–800	14–26	
DW-EPI	10000	91–93	
ADC	10000	91–93	
PD	3800–4440	13–15	

FLAIR, fluid attenuation inversion recovery; DW-EPI, diffusion weighted echo-planar images; ADC, apparent diffusion coefficient images; GRE, gradient echo; PD, proton density.

heterogeneous enhancement. On T2∗gradient echo (T2∗GRE) images masses were isointense or hyperintense relative to normal gray matter; one of the masses (cat #2) had a central susceptibility artifact on T2∗GRE images. Masses were hyperintense relative to adjacent parenchyma on diffusion weighted echo planar imaging (DW-EPI) and isointense on apparent diffusion coefficient images (ADC). The masses of cat #1, 2, 4, and 5 were fairly homogeneous. The largest mass, cat #3, had multifocal cavitations, which were hyperintense on T2W (isointense to CSF), mildly hypointense on T2W-FLAIR, hypointense on T1W, and nonenhancing, consistent with fluid filled cavities and/or necrosis (Fig. 2).

All cats had evidence of obstructive hydrocephalus, characterized by bilateral moderate to severe dilation of the lateral ventricles and unilateral or bilateral dilation of the olfactory recesses. Hydrocephalus and subsequent mass effect

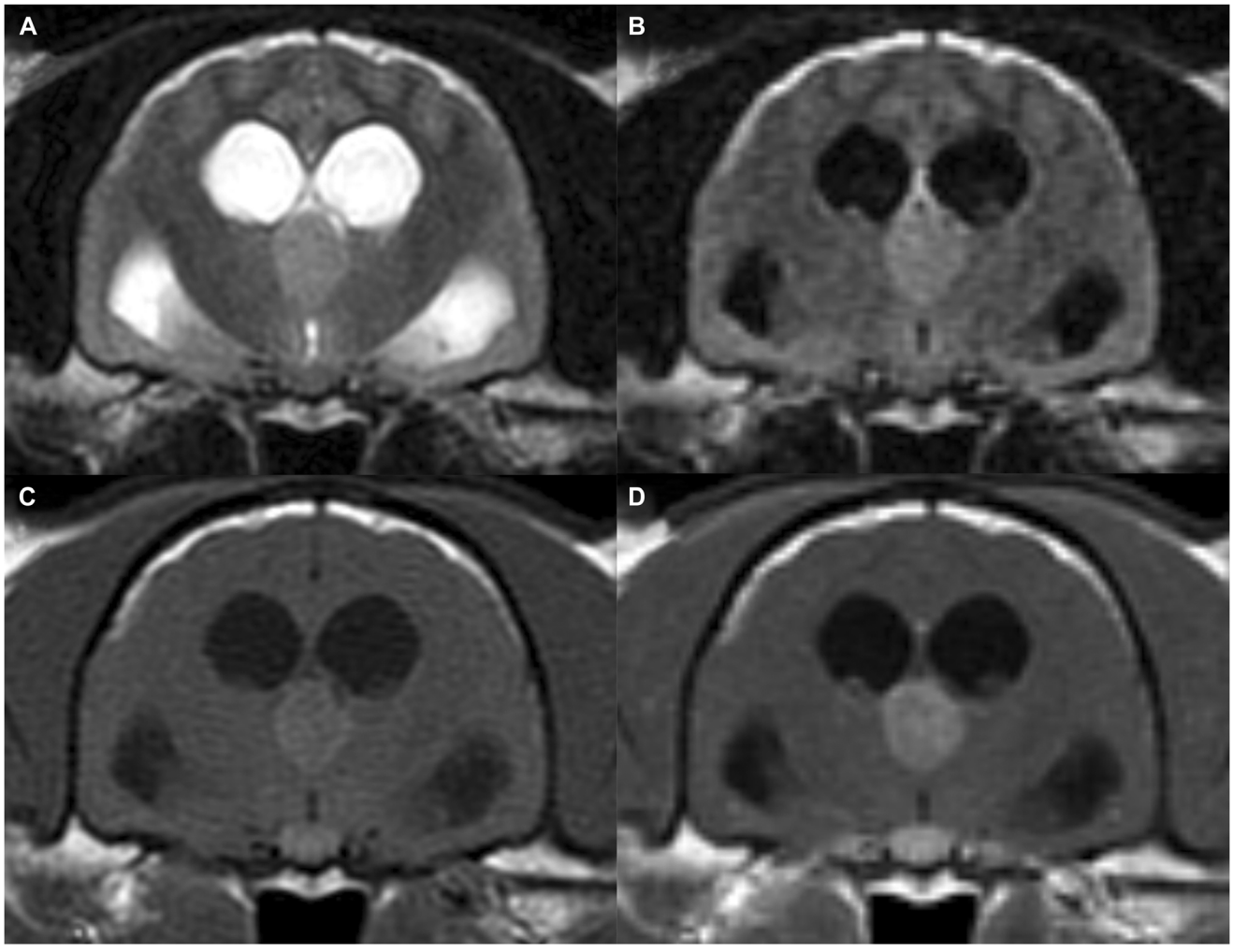

Fig. 1. Transverse T2W (A), T2W-FLAIR (B), and T1W pre- (C) and postcontrast (D) images of an intraventricular ependymoma in a 9-year-old, spayed female, domestic shorthaired cat (cat #4). In the dorsal aspect of the third ventricle there is an ovoid mass which is hyperintense on T2W (A), T2W-FLAIR (B), and T1W (C) images and has strong, homogeneous contrast enhancement (D). Both lateral ventricles are symmetrically moderately distended, consistent with hydrocephalus. There is also loss of visualization of the CSF in the subarachnoid space around the brain and within the sulci on the T2W image.

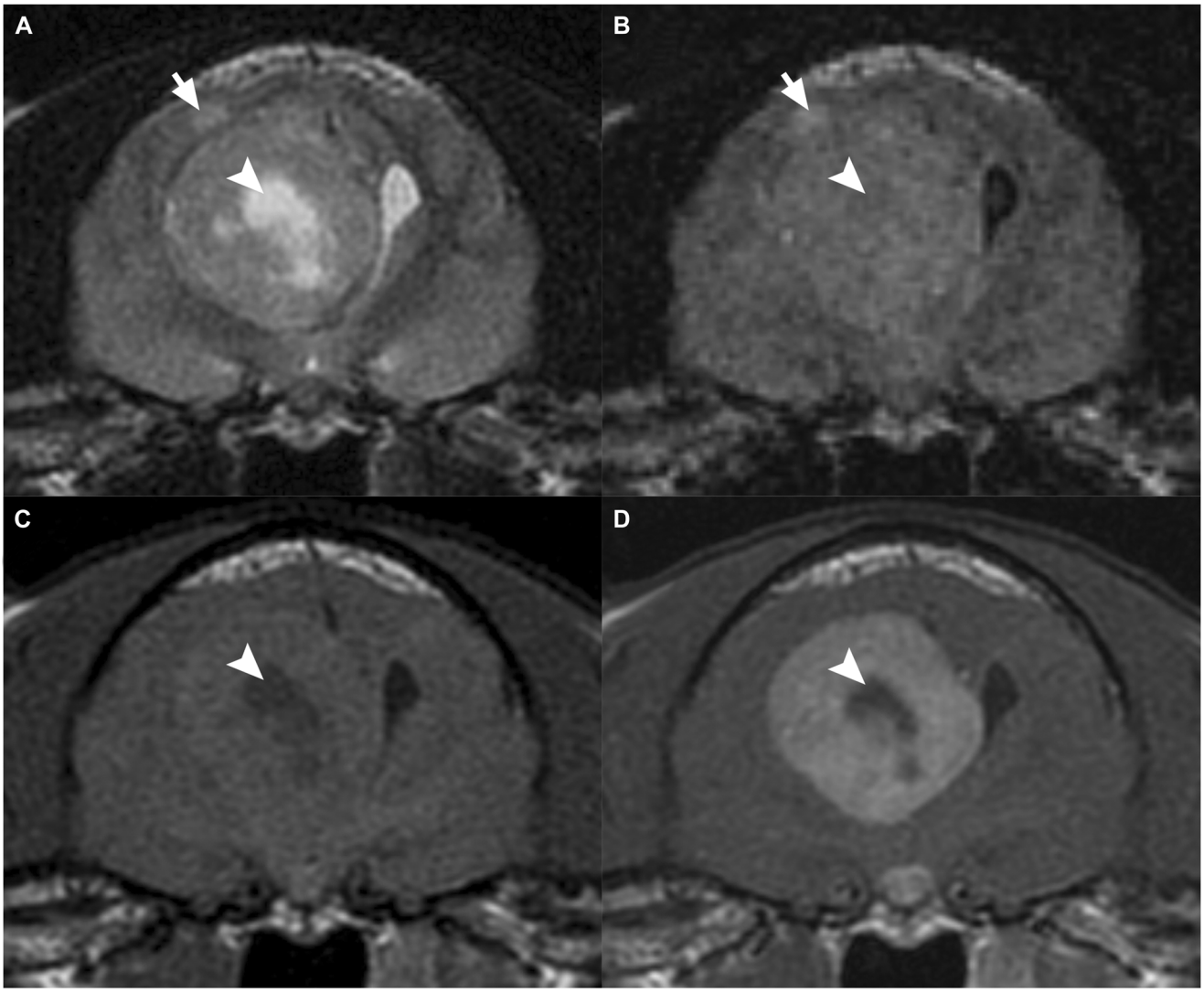

FIG. 2. Transverse T2W (A), T2W-FLAIR (B), and T1W pre- (C) and postcontrast (D) images of an intraventricular ependymoma in a 5-year-old, male castrated, domestic longhaired cat (cat #3). In the right ventricle near the level of the intraventricular foramen there is a spherical mass that is hyperintense on T2W (A) and T2W-FLAIR (B) images, isointense to mildly hyperintense T1W (C) on the image, and strongly contrast enhancing (D). There are cavitations within the mass (arrow head), which are hyperintense on T2W images (isointense to CSF), mildly hypointense on T2W-FLAIR images, hypointense on T1W images, and noncontrast enhancing. There is mild dilation of the left lateral ventricle and a midline shift to the left. Perilesional edema is seen as a focal hyperintensity on T2W and T2W-FLAIR images in the brain parenchyma adjacent to the mass (arrow). Edema extended rostral to the mass along the ipsilateral white matter of the internal capsule and corona radiata (not shown). On the T2W image there is loss of visualization of the CSF in the subarachnoid space around the brain and within the sulci.

resulted in unilateral or bilateral caudal transtentorial herniation of the occipital lobes with or without involvement of the lateral ventricles, cerebellar herniation through the foramen magnum, and loss of visualization of CSF in the subarachnoid space on T2W images. Parenchymal herniation resulted in compression of the mesencephalon, cerebellum, and medulla oblongata. Subfalcine herniation, defined as any shift from midline, was appreciated in 4/5 cats. Periventricular hyperintensity was present on T2W / T2W-FLAIR images along the herniated portions of the lateral ventricles, consistent with interstitial edema/transependymal CSF flow. Parenchymal perilesional edema was present adjacent to the masses of cat #1, 2, 3, and 5, and was questionable in cat #4. Perilesional edema was most severe in cat #3, with T2W hyperintensity extending along the ipsilateral white matter of the internal capsule and corona radiata.

On T2W-FLAIR images, inadequate suppression of CSF was noted in 2/5 cats; however, this was suspected to be an artifact associated with MRI technique given the presence of similar lack of suppression of aqueous/vitreous components of the eye on those images (T2W-FLAIR parameters with inadequate fluid suppression: repetition time 9000 ms, echo time 78 ms, inversion time 2500 ms; T2W-FLAIR

parameters with suitable fluid suppression: repetition time 8002 ms, echo time 117–131 ms, inversion time 2000 ms).

Outcome

Lateral ventricular trephination was performed in cat #1. Cerebrospinal fluid obtained by trephination was evaluated; the sample was hemodilute and nondiagnostic. Brainstem auditory evoked response (BAER) testing performed in cat #1 indicated loss of brainstem function. Cat #1, 4, and 5 were humanely euthanized the same day as their MRI due to poor prognosis. Cat #3 was initially discharged, but represented 3 days after the MRI for progressively dull mentation, inability to stand, and intermittent decerebrate posturing. A rostrotentorial craniotomy was performed the same day in an attempt to remove the mass and relieve intracranial pressure. The cat failed to recover following surgery and was euthanized later that night. Cat #2 was discharged with medical management, including prednisolone (Henry Schein Animal Health, Dublin, OH), gabapentin (Neurontin, Pfizer, Parke-Davis, New York, NY), and omeprazole (Dexcel Pharma Technologies Ltd., Yokneam, Isreal) which provided mild improvement in clinical signs. A ventriculoperitoneal shunt was placed 6 days after the MRI. Following shunt placement, cat #2 showed immediate improvement in neurologic status and mobility. Six months following shunt placement clinical signs of aggression toward the housemate, head tremors, decreased activity, inappropriate urination, and anorexia developed. Ten months following the MRI the cat represented for humane euthanasia due to progressive worsening of clinical signs and poor prognosis.

Histopathology of the intraventricular mass was performed in all cats, and all were consistent with ependymomas. The mass in cat #3 was further subclassified as a papillary ependymoma. The largest cavitation in this mass corresponded to necrosis. Smaller cavitations were associated with additional areas of necrosis, ectatic vessels, lakes of eosinophilic proteinaceous fluid, and/or edematous stroma separating neoplastic cells. Antemortem biopsy of the mass in cat #3 was in agreement with the postmortem histopathology. The mass in cat #2 was determined to be malignant based on local microscopic invasion and mitotic index. This cat also had minimal, multifocal perivascular lymphocytic encephalitis. The mass in cat #5 had a few scattered areas of necrosis. Hemorrhage was noted within with the mass of cat #1, and within the brain parenchyma of cat #1 and 3. Cat #1 had extensive encephalomalacia of the cerebellum and brainstem. Histopathology in cat #4 was limited to the intraventricular mass. No evidence of metastasis was found in any of the cats for which a full necropsy was performed. Portions of brain tissue were submitted for rabies testing in 2/5 cases; results were negative.

Discussion

To the authors' knowledge, this is the first published report describing the MRI features of intraventricular ependymomas in the brains of cats with neurologic signs. Other differential diagnoses for neoplastic masses within the ventricular system of the brain include choroid plexus tumor (papillomas, carcinomas), meningioma, lymphoma, and less likely astrocytoma.[2,3,8,12,13] Histiocytic sarcoma within the subependymal region of the lateral ventricle has also been reported in a single cat.[14] Congenital malformations, granulomas, hemorrhage, hematomas, and abscesses are also possible.[8,13] Similar to the five cats in this case series, cats with ependymomas typically present with neurologic signs (altered mentation and behavior, circling, propulsive gait, head pressing, decreased or absent menace response, and seizures).[2,3,5–7,11] In all five cats, neurologic signs were thought to be secondary to obstructive hydrocephalus and brain herniation, likely due to the location of the masses within the third ventricle or near the interventricular septum.

Many commonalities were identified between the imaging characteristics of the five ependymomas in this study. The ependymomas were all hyperintense compared to normal gray matter on T2W, T2W-FLAIR, and proton density images. Variability was seen in the T2∗GRE and T1W images, with masses being isointense to hyperintense compared to normal gray matter on these sequences. Contrast enhancement was strong and homogeneous in most of the cases, but in one cat, enhancement was more subtle and heterogeneous. In the cases where DW-EPI and ADC images were available, the masses were hyperintense to adjacent parenchyma on DW-EPI and isointense on ADC consistent with the masses being composed of areas of increased cellularity.[15,16] The imaging characteristics of the malignant ependymoma were not definitively distinguishable from those in the other cases.

In dogs, ependymomas are reported to be heterogeneously T2W hyperintense, hyperintense on DWI, and T1W hypointense to slightly hyperintense in relation to normal gray matter. Contrast enhancement is usually strong and heterogeneous, however, one dog was reported to have no contrast enhancement.[4,17,18] In humans, in relation to normal gray matter, ependymomas are T2W isointense to hyperintense, T1W isointense to hypointense, have heterogeneous contrast enhancement, and can have variable findings on diffusion-weight images.[8]

A cause for hyperintensity on T1W images in the ependymomas of this study was not determined, because there were no findings concurrent to these on histopathologic examination. In general, hyperintensity on precontrast T1W images has been associated with hemorrhage, protein-containing lesions, fat, melanin, vasopressin, calcification/mineral, and potentially myelin degradation

products.[19] Histopathologically, ependymomas may have cyst-like areas representing areas of necrosis or fluid accumulation, while others may have mineralization, cholesterol clefts and/or hemorrhage, which contribute to heterogeneity on MRI.[2,3,5,6] While hemorrhage was present histopathologically in the masses and brain parenchyma of cat #1 and 3, this was not identified with MRI and was likely secondary to procedures (lateral ventricular trephination and craniotomy/encephalotomy, respectively) performed after the MRI studies were acquired. The T2∗GRE hypointense focus/susceptibility artifact in the mass of cat #2 may be consistent with hemorrhage; however, the presence of hemorrhage was minimal to absent according to the necropsy report.

The imaging characteristics of ependymomas in this study can be compared to other intraventricular neoplasms, such as meningiomas and choroid plexus tumors. In dogs and cats compared to normal grey matter, meningiomas are typically hyperintense relative to normal gray matter on T2W images and uniformly iso- to hypointense relative to normal gray matter on T1W images with marked, uniform contrast enhancement. In older cats, multiple meningiomas may be present simultaneously.[3,4,17,20,21] In dogs, choroid plexus tumors are usually T2W hyperintense in relation to normal gray matter, may be T1W hypo-, iso-, or hyperintense in relation to normal gray matter, and have marked uniform contrast enhancement. They often appear heterogeneous due to intratumoral hemorrhage.[4,17,20]

In conclusion, the current study summarized MRI characteristics of confirmed intraventricular ependymomas in a sample of five cats. Further studies would be needed to assess specificity of the imaging characteristics reported versus other intraventricular neoplasms, but this study highlighted some common imaging features and supported the inclusion of this tumor type when considering intraventricular masses in feline patients.

LIST OF AUTHOR CONTRIBUTIONS

Category 1

(a) Conception and Design: Antonia DeJesus, Jantra N. Suran
(b) Acquisition of Data: Antonia DeJesus, Eli B. Cohen, Jantra N. Suran
(c) Analysis and Interpretation of Data: Antonia DeJesus, Eli B. Cohen, Evelyn Galban, Jantra N. Suran

Category 2

(a) Drafting the Article: Antonia DeJesus, Jantra N. Suran
(b) Revising Article for Intellectual Content: Antonia DeJesus, Eli B. Cohen, Evelyn Galban, Jantra N. Suran

Category 3

(a) Final Approval of the Completed Article: Antonia DeJesus, Eli B. Cohen, Evelyn Galban, Jantra N. Suran

Appendix 1: Clinical Findings for Five Cats with Intraventricular Ependymomas

Cat	Signalment	Duration of signs	Clinical signs	Diagnostic tests	Time from MRI to necropsy	Location of mass	Histopathologic diagnosis
1	4 years FS DLH	<1 day	Acute nonambulatory tetraparesis; respiratory arrest	CBC, biochemistry panel, urinalysis; tests for FeLV, FIV toxoplasma, and feline coronavirus; thoracic and cervical radiographs; CSF analysis (hemodilute); BAER testing (loss of brainstem function)	<1 day	Left lateral ventricle ± third ventricle	Ependymoma
2	4.5 years FS DSH	2 months	Behavioral changes; vestibular ataxia; weakness; crouched stance; positional nystagmus; progressive lethargy; anorexia; weight loss	CBC (neutropenia); biochemistry panel; tests for FeLV and FIV; coagulation panel; bile acids; blood ammonia; urinalysis (1+ protein); thoracic radiographs; abdominal ultrasound (subjectively hypoechoic liver, mild jejunal muscularis thickening); liver FNA	10 months	Third ventricle	Malignant ependymoma
3	5 years MC DLH	2 months	Progressive lethargy; dull mentation; aimless walking; circling to the right; left proprioceptive deficits; absent menace OS, decreased left palpebral reflex and facial sensation	CBC, biochemistry panel; tests for FeLV and FIV; thoracic radiographs	3 days	Right lateral ventricle	Ependymoma, papillary subtype
4	9 years FS DSH	1 week	Dull mentation; positional rotary nystagmus; increased muscle tone in all limbs; circling to the right	CBC (mild neutrophilia, mild thrombocytopenia), biochemistry panel; tests for FeLV, FIV and toxoplasma; rabies (postmortem)	<1 day	Third ventricle	Ependymoma

Cat	Signalment	Duration of signs	Clinical signs	Diagnostic tests	Time from MRI to necropsy	Location of mass	Histopathologic diagnosis
5	10 years MC DSH	1.5 week	Behavioral changes (restless, pacing, hiding); stargazing; suspected seizure; positional nystagmus (vertical); crouched stance; vesitibular ataxia; anorexia	CBC (mild neutropenia), biochemistry panel; tests for FeLV, FIV, toxoplasma, and heartworm; thoracic radiographs; abdominal ultrasound (subjectively hyperechoic liver); liver FNA	2 days	Third ventricle	Ependymoma

Diagnostics performed were unremarkable, unless otherwise noted.
FS, female, spayed; MC, male, castrated; DLH, domestic longhair cat; DSH, domestic shorthair cat; CBC, complete blood count; FeLV, feline leukemia virus; FIV, feline immunodeficiency virus; CSF, cerebrospinal fluid; BAER, brainstem auditory evoked response; FNA, fine needle aspirate.

Appendix 2: Magnetic Resonance Imaging Findings in Five Cats with Intraventricular Ependymomas

Cat Mass location	1 Left lateral ventricle ± third ventricle	2 Third ventricle	3 Right lateral ventricle	4 Third ventricle	5 Third ventricle
Mass dimensions, mm (L × W × H)	6.1 × 9.0 × 4.2	14.6 × 6.2 × 10	19.5 × 17.5 × 17.4	12.6 × 7.1 × 10.4	15.2 × 7.5 × 9.4
Shape	Ovoid	Ovoid	Spherical	Ovoid	Ovoid
Intralesional cavitations	No	No	Yes	No	No
T2W	Hyperintense	Hyperintense	Hyperintense	Hyperintense	Hyperintense
PD	N/A	Hyperintense	N/A	N/A	Hyperintense
T2W-FLAIR	Hyperintense	Hyperintense	Hyperintense	Hyperintense	Hyperintense
T2*GRE	Isointense	Hyperintense with a hypointense focus†	Hyperintense	N/A	Hyperintense
T1W	Isointense	Isointense to mildly hyperintense	Isointense to mildly hyperintense	Hyperintense	Hyperintense
Contrast enhancement	Strong, homogeneous	Strong, homogeneous	Strong, homogeneous	Strong, homogeneous	Mild, heterogeneous
DW-EPI	Hyperintense	N/A	Hyperintense	Hyperintense	N/A
ADC	Isointense	N/A	Isointense	Isointense	N/A
Suppression of CSF on T2W-FLAIR	Complete	Incomplete‡	Complete	Complete	Incomplete†
Perilesional edema	Mild	Mild	Moderate	Questionable	Mild
Obstructive hydrocephalus					
Lateral ventricular dilation	Severe Lt; mild Rt	Severe bilateral (Rt > Lt)	Moderate bilateral	Severe bilateral (Rt > Lt)	Severe bilateral (Rt > Lt)
Olfactory recess dilation	Severe Lt; mild Rt	Severe bilateral (Lt > Rt)	Moderate Lt	Severe bilateral (Rt > Lt)	Moderate Rt
Brain herniation					
Transtentorial herniation	Rt occipital lobe, (questionable Lt occipital lobe); Rt lateral ventricle	Bilateral occipital lobes and lateral ventricles	Bilateral occipital lobes; Rt lateral ventricle	Bilateral occipital lobes and lateral ventricles	Bilateral occipital lobes and lateral ventricles
Foramen magnum herniation	Yes	Yes	Yes	Yes	Yes
Subfalcine herniation	Right midline shift	No	Left midline shift	Minimal left midline shift	Mild left midline shift

**Signal intensities are relative to normal gray matter.
L, rostrocaudal length; W, mediolateral width; H, dorsoventral height; Rt, right; Lt, left; >, greater than; N/A, not applicable.
†Attributed to susceptibility artifact.
‡Incomplete suppression of CSF suspected due to artifact from imaging technique.

REFERENCES

1. Koestner A, Higgins RJ. Tumors of the nervous system. In: Meuten D (ed): Tumors in domestic animals, 4th ed. Ames, IA: Iowa State Press, 2008;697–738.

2. Tremblay C, Girard C, Quesnel A, Thorneloe C, Belanger J-F. Ventricular ependymoma in a cat. Can Vet J 1998;39:719–720.

3. Troxel MT, Vite CH, Winkle TJ, et al. Feline intracranial neoplasia: retrospective review of 160 cases (1985–2001). J Vet Intern Med 2003;17(6):850–859.

4. Wisner E, Zwingenberger A. Neoplasia. In: Atlas of small animal CT and MRI. Ames, IA: John Wiley & Sons, 2015;221–243.

5. Woolford L, de Lahunta A, Baiker K, Dobson E, Summers B. Ventricular and extraventricular ependymal tumors in 18 cats. Vet Pathol 2013;50:243–251.

6. Zaki FA, Hurvitz AI. Spontaneous neoplasms of the central nervous system of the cat. J Small Anim Pract 1976;17:773–782.

7. Simpson D, Hunt G, Tisdall P, et al. Surgical removal of an ependymoma from the third ventricle of a cat. Aust Vet J 1999;77:645–648.

8. Smith AB, Smirniotopoulos JG, Horkanyne-Szakaly I. Intraventricular neoplasms: radiologic-pathologic correlation. Radiographics 2013;33: 21–43.

9. Fox JG, Snyder SB, Reed C, Campbell LH. Malignant ependymoma in a cat. J Small Anim Pract 1973;14:23–26.

10. Cherubini GB, Mantis P, Martinez TA, Lamb CR, Cappello R. Utility of magnetic resonance imaging for distinguishing neoplastic from non-neoplastic brain lesions in dogs and cats. Vet Radiol Ultrasound 2005;46: 384–387.

11. de Lahunta A, Glass E. Cerebrospinal fluid and hydrocephalus. In: Glass AdL (ed): Veterinary neuroanatomy and clinical neurology, 3rd ed. Saint Louis: W.B. Saunders, 2009;54–76.

12. Vandevelde M, Higgins R, Oevermann A. Neoplasia. In: Veterinary neuropathology: essentials of theory and practice. Hoboken, NJ, USA: John Wiley & Sons, 2012;129–156.

13. Glastonbury CM, Osborn AG, Salzman KL. Masses and malformations of the third ventricle: normal anatomic relationships and differential diagnoses. Radiographics 2011;31:1889–1905.

14. Ide T, Uchida K, Tamura S, Nakayama H. Histiocytic sarcoma in the brain of a cat. J Vet Med Sci 2010;72:99–102.

15. Koh D-M, Collins DJ. Diffusion-weighted MRI in the body: applications and challenges in oncology. Am J Roentgenol 2007;188: 1622–1635.

16. Provenzale JM, Mukundan S, Barboriak DP. Diffusion-weighted and perfusion MR imaging for brain tumor characterization and assessment of treatment response. Radiology 2006;239: 632–649.

17. Kraft SL, Gavin PR, DeHaan C, Moore M, Wendling LR, Leathers CW. Retrospective review of 50 canine intracranial tumors evaluated by magnetic resonance imaging. J Vet Intern Med 1997;11: 218–225.

18. Vural SA, Besalti O, Ilhan F, Ozak A, Haligur M. Ventricular ependymoma in a German Shepherd dog. Vet J 2006;172:185–187.

19. Cakirer S, Karaarslan E, Arslan A. Spontaneously T1-hyperintense lesions of the brain on MRI: a pictorial review. Curr Probl Diagn Radiol 2003;32:194–217.

20. Wisner ER, Dickinson PJ, Higgins RJ. Magnetic resonance imaging features of canine intracranial neoplasia. Vet Radiol Ultrasound 2011;52(1 Suppl 1):S52–S61.

21. Motta L, Mandara MT, Skerritt GC. Canine and feline intracranial meningiomas: an updated review. Vet J 2012;192:153–165.